Global Ecology and Conservation 43 (2023) e02442

Contents lists available at ScienceDirect

Global Ecology and Conservation

journal homepage: www.elsevier.com/locate/gecco

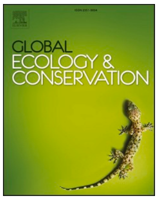

Species Distribution Models predict abundance and its temporal variation in a steppe bird population

Alice Monnier-Corbel [a,d,*], Alexandre Robert [b], Yves Hingrat [d], Blas M. Benito [c], Anne-Christine Monnet [b]

[a] *Emirates Center for Wildlife Propagation, PO Box 47, 33250 Missour, Morocco*
[b] *Centre d'Ecologie et des Sciences de la Conservation (CESCO), Muséum National d'Histoire Naturelle, Centre National de la Recherche Scientifique, Sorbonne Université, CP 135, 57 rue Cuvier, 75005 Paris, France*
[c] *Instituto Multidisciplinar para el Estudio del Medio "Ramon Margalef", Universidad de Alicante, Carretera de San Vicente del Raspeig s/n, San Vicente del Raspeig Alicante 03690, Spain*
[d] *RENECO International Wildlife Consultants LLC, PO Box 61741, Abu Dhabi, United Arab Emirates*

ARTICLE INFO

Keywords:
Abundance
Habitat suitability
Niche model
Houbara
Population dynamics

ABSTRACT

Habitat Suitability Index (HSI) derived from Species Distribution Model (SDM) has been used to infer or predict local demographic properties such as abundance for many species. Across species studied, HSI has either been presented as a poor predictor of abundance or as a predictor of potential rather than realized abundance. The main explanation of the lack of relationship between HSI and abundance is that the local abundance of a species varies in time due to various ecological processes that are not integrated into correlative SDM. To better understand the HSI-abundance relationship, in addition to the study of the association between HSI and mean abundance, we explored its variation over time. We used data from 10-years monitoring of a Houbara bustard (*Chlamydotis undulata undulata*) population in Morocco. From various occurrence data we modelled the HSI. From (independent) count data we calculated four local abundance indices: mean abundance, maximum abundance, the temporal trend of abundance and the coefficient of variation of abundance over the study period. We explored the relationship between HSI and abundance indices using linear, polynomial and quantile regressions. We found a triangular relationship between local abundance (mean and maximum) and HSI, indicating that the upper limit of mean and maximum abundance increased with HSI. Our results also indicate that sites with the highest HSI were associated with least variation in local abundance, the highest variation being observed at intermediate HSI. Our results provide new empirical evidence supporting the generalization of the triangular relationship between HSI and abundance. Overall, our results support the hypothesis that HSI obtained from SDMs can reflect the local abundance potentialities of a species and emphasize the importance of investigating this relationship using temporal variation in abundance.

1. Introduction

Abundance is a key demographic property that allows making diagnoses on population dynamics. However, in many plants and

---

[*] Corresponding author at: Emirates Center for Wildlife Propagation, PO Box 47, 33250 Missour, Morocco.
E-mail address: alice.monnierc@orange.fr (A. Monnier-Corbel).

https://doi.org/10.1016/j.gecco.2023.e02442
Received 2 January 2023; Received in revised form 28 February 2023; Accepted 24 March 2023

animals, measuring the abundance of a species requires a significant sampling effort that is costly and not always feasible at large spatial scales. Hence, abundance data remain rare for many species, including threatened species (Cardoso et al., 2012; Bachman et al., 2019; Cowie et al., 2022). Species distribution models (hereafter, SDM), which offer the advantage of using only occurrence data, constitute the only basis for conservation status assessment in many species (Cardoso et al., 2012; Régnier et al., 2015). Here, we define SDMs as correlative models that relate species occurrence data to environmental variables. We include the various nomenclatures that exist in the literature to define these models (e.g. ecological niche model, ENMs), but we exclude mechanistic or process-based SDMs (Kearney and Porter, 2009). By combining species occurrences and large-scale environmental variables (Elith and Leathwick, 2009), these models estimate an index of habitat suitability (hereafter, HSI) that should reflect the spatial variability of the quality of the habitat for that species. SDMs can also be used at other scales of biological integration such as taxa or ecosystem (Svenning et al., 2011; Carnaval and Moritz, 2008). Theoretically, under ideal circumstances (i.e., a SDM modeled with representative species occurrences and suitable environmental data), a relationship is expected between the HSI and spatial variation in demographic parameters (such as breeding success and survival, Monnet et al., 2015; Bacon et al., 2017) and demographic properties (such as the growth rate or abundance, Brown, 1984; VanDerWal et al., 2009). Hence, there is a growing interest in studying the relationship between HSI and abundance to better understand the relevance of SDM in ecology and conservation. A relationship between HSI and abundance could indeed be useful when the objective is to make inferences on abundance at a broad spatial scale (Van Couwenberghe et al., 2013) or to set conservation priorities. For example, HSI distribution maps could be used to plan translocation actions, habitat restoration, and site protection actions (Osborne and Seddon, 2012; IUCN/SSC, 2017).

However, a recent review showed contrasted and complex relationships between HSI and abundances (Lee-Yaw et al., 2022). The uncertainty associated with the SDM methodology could impact the strength of the relationship between HSI and abundances, either through the variability in SDM modeling methods (Ready et al., 2010; Tôrres et al., 2012), the choice of environmental predictors selected for modeling (Weber et al., 2017) or the implementation of SDM on multiple species and/or small sample size (Lee-Yaw et al., 2022). In addition, spatial and temporal scale constraints are not always accounted for in the large-scale climate predictors often used in SDM (Bean et al., 2014; Baer and Maron, 2020). But overall, SDM are simple correlative models that do not take into account the processes that determine site abundance, such as resource availability and biotic interactions. Two main types of biological mechanisms may explain the temporal variation in abundance of a population at a specific site: 1) the intrinsic growth rate of the population, linked to the survival and reproduction parameters of the population in relation with the habitat, 2) the dispersal of individuals (emigration and immigration), which can vary according to a variety of ecological processes such as density-dependence, source-sink dynamics, habitat selection, natal or breeding dispersal, and seasonal movements. All these processes may contribute to deviations from the expected relationship between HSI and abundance (VanDerWal et al., 2009), and their relative importance on abundance variation depends on the spatial scale and the species considered (Brown et al., 1995; Kneitel and Chase, 2004).

Several studies showed that such sources of temporal variation in local abundance generally lead to a triangular relationship between realized abundance and HSI (VanDerWal et al., 2009; Tôrres et al., 2012; Acevedo et al., 2017; Carrascal et al., 2017; Jimenez-Valverde et al., 2021), i.e., sites of low HSI are associated with low abundances while sites of high HSI are associated to either low, intermediate or high abundances. Therefore, several authors suggested that SDM could be useful for identifying the potential (but not necessary) realized abundance at a specific location (VanDerWal et al., 2009), also referred as carrying capacity. The carrying capacity of an environment is a key ecological concept with important implications for species conservation and restoration (McKeon et al., 2009; Guyondet, 2015). It refers to the maximum population size of a species that can be maintained by a specific environment, given the resources available to the species (Verhulst, 1838). The habitat suitability is a critical component of carrying capacity and its spatial variation (Downs et al., 2008). In favorable habitats, higher carrying capacities and higher growth rates are expected compared to less favorable habitats. Thus, HSI would be closer to predictions of maximum abundance at a given site than to the abundance observed at a particular time, and could be appropriate tools to estimate the carrying capacity of an environment (Downs et al., 2008; Liu et al., 2017). However, for reasons explained above, the abundance of a species at a given site may exhibit large temporal abundance variation below its carrying capacity. A proper estimate of carrying capacity would then require long term abundance data sets and analysis focusing on the temporal patterns of the HSI-abundance relationship.

To our knowledge, only few studies have focused on the temporal pattern of the HSI-abundance relationship. Thuiller et al. (2014) found negative relationship between intrinsic population growth rate and HSI. Acevedo et al. (2017) used the triangular relationship framework to compare a large number of increasing roe deer (*Capreolus capreolus*) populations (each monitored in two separate periods). Their results indicated that the abundance deficit predicted by the triangular relationship in the first period of monitoring was positively correlated with the local population growth rate between the two periods, suggesting that HSI can be used as a proxy for carrying capacity. More recently, Regos et al. (2021) observed a positive relationship between abundance and HSI, but changes in HSI did not explain temporal variation in local abundances.

Here we take advantage of 10 years monitoring of a population of Houbara bustard (*Chlamydotis undulata undulata*), a steppe bird of North Africa. This population provides an optimal study system to test the relationship between abundances and the outcomes from SDM, thanks to sizeable and distinct data sets. Using occurrence data, we modelled the niche of the Houbara bustard population during the fall season and investigated the relationship between HSI and local abundances, estimated from fall count data. We then examined linear and non-linear relationships between local abundances and HSI, using the local mean abundance and the coefficient of abundance variation, the trend in abundance and the maximum abundance computed over the 10-year study period. We predict a triangular relationship between mean and maximum local abundance and habitat suitability index, and less abundance variation in best sites. As the Houbara bustard population shows no clear global trend over the study period (clear positive or negative trend) in the study area (Monnier-Corbel et al., 2021), we do not have a precise prediction for the relationship between local temporal trend and HSI in contrast to the work of Acevedo et al. (2017) which focused on increasing populations.

2. Methods

2.1. *Species and study area*

The North African Houbara bustard (*Chlamydotis undulata undulata*, here-after "houbara") is a medium-sized bird living in arid to semi-arid environments with open and sparse vegetation (Hingrat et al., 2007). The historical range of the houbara covers North Africa, from northern Mauritania to Egypt. Since the 1980 s, the houbara population has declined severely (Goriup, 1997) due to unregulated hunting, poaching and habitat degradation (Lacroix et al., 2003). The species is classified as vulnerable (BirdLife International, 2016). Its decline led to the establishment in 1995 in Morocco of a conservation programme, the Emirates Center for Wildlife Propagation (ECWP, Lacroix et al., 2003). The comprehensive approach of ECWP combines conservation translocation (reinforcement of wild population with captive-bred individuals) and in situ measures such as awareness, protection, and hunting regulation.

Our study area is the primary intervention area of the ECWP in Morocco, the Eastern region (approximatively 50,000 km^2; see Fig. 1). Captive-bred individuals are released throughout the year both in hunted and non-hunted areas (Hardouin et al., 2015; Monnier-Corbel et al., 2021). A total of 11,344 individuals were released between 1998 and 2020. The annual abundance of houbara in the study area between 2011 and 2020 was estimated at around 16,918 ± 1875 houbaras, corresponding to an average density of 0.44 ± 0.05 houbara per km^2 (Monnier-Corbel et al., 2021).

2.2. *Abundance*

2.2.1. *Abundance estimation*

A counting protocol using standardized circular point observations is carried out each fall (from September to December) on the Eastern region (see Monnier-Corbel et al., 2021 for details on counting points protocol). In the present study, we used the count data from 2011 to 2020 (Appendix S1).

The count data were used to model a detection function using the distance sampling method (Buckland and Elston, 1993). This method assumes that the probability of detection decreases as its distance from the observer increases. Then, we applied Density Surface Modelling (hereafter, "DSM") to spatialize abundance estimates from distance sampling data (Miller et al., 2013; see Monnier-Corbel et al., 2021 for details in DSM). We restricted the prediction grid to the areas favorable to the presence of houbara in the study area, excluding mountainous areas with a slope greater than 5%, and urban areas. The prediction grid in the Eastern region represented a total of 38,575 km^2 (77% of the 50,170 km^2 of the study area), with 878 pixels of 73.27 km^2 (grid of 5 min of arc). We fitted a Generalized Additive Model to model the average and annual estimate of houbara abundance as a function of geographic coordinates using a Tweedie response distribution to tune model flexibility (Miller et al., 2013). This step resulted in annual maps of abundance distribution from 2011 to 2020 (ten maps of 878 pixels each) with their uncertainty (coefficient of variation).

2.2.2. *Abundance indices*

We calculated each abundance index from estimates of the annual maps of abundance distribution. Each map pixel was associated with an ID and its abundance and uncertainty estimates for each year. Then, for each pixel ID, we: (1) calculated the mean of the annual abundances (mean abundance); (2) identified the maximum abundance value between the different annual estimates (max abundance); (3) performed a linear regression between the log-transformed abundances and time (year as a quantitative variable), using the regression slope as a temporal trend value; (4) calculated a coefficient of variation of abundance from the annual abundances (i.e. the ratio of standard deviation to mean).

2.3. *Habitat Suitability Index*

2.3.1. *Presence data*

To model the suitable habitat of the population (including wild-born and captive-born houbara), we used presence records collected by the ECWP conservation programme. We used different types of geolocalized presence data: tracking locations of wild-born and captive-born individuals (equipped with transmitters or VHF; Hardouin et al., 2015; Bacon, 2017), and any occasional observations (see Appendix S2 for details on occurrences data). We only used the presence data recorded during the counting season (from September to December) and thus modelled the suitable habitat in fall season. We discarded all positions of young captive-born individuals ($<$ 1-year-old) to focus on settled individuals. We assigned the presence data to the resolution of the environmental predictors, i.e. $\sim$1 km^2 grid cells (see section Environmental data). The number of presence records in each grid cell varied widely, from one unique presence to multiple observations over time. For each grid cell, we thus computed the number of weeks of observed presences to be used as relative sampling probabilities of training cases in random forest models. The number of presence weeks ranged from 0.142 (one day) to 68.85 weeks. To avoid inflating the weight of grid cells where the observation programme has been running for a longer time, we ran a sensitivity analysis to find a meaningful threshold for the maximum training weight. We set it to the quantile 0.25 of the maximum number of observed weeks (2.29 weeks). We then thinned the occurrences by imposing a minimum separation of two grid cells between nearby records and preferentially selecting the pixels with higher weights. In the end, we accumulated a total of 3800 weighted presence grid cells.

2.3.2. *Background data*

Due to a lack of absence data we used background data and then modelled *use* versus *availability* of habitat rather than *presence* versus *absence* of the birds (Boyce and McDonald, 1999; Gianpasquale, 2017). When modeling use versus availability, the presence data represents habitat use, while the background data represents availability. To generate an ecologically meaningful background dataset, we first computed a convex hull around the presence records. We then calculated the maximum possible distance between two presence records (~1540 km) and used it as a radius to define a buffer around the convex hull enclosing the presence data. The region inside the buffer represented all the areas and ecological conditions the population has potential access to. We then randomly selected 10,000 background points within this area. The case weight for each background record was set to 0.14, corresponding to the sum of weights of all the presences divided by 10,000.

2.3.3. Environmental data

We prepared fifty-one environmental predictors from diverse sources at a 1 km resolution (Appendix S3). To select non-collinear predictors, we ranked them by their median permutation importance across thirty Random Forest models using the function *rf_repeat* in the R package *spatialRF* (Benito, 2021), with the weighted presence and background data as response variable against the fifty-one predictors. This approach ensures the robustness of predictor ranking to the stochasticity inherent in the Random Forest algorithm. We then removed predictors one by one in decreasing order of importance until their variance inflation factors were equal to or lower than five (following O'brien, 2007) and their maximum Pearson correlation with any other variable was 0.75 or lower (following the recommendation of Fox and Monette, 1992). We thus obtained a set of predictors not correlated among themselves with the maximum explanatory power.

2.3.4. Modelling

We fitted and analyzed a Random Forest model with the R package *ranger* (Wright and Ziegler, 2015) via the R package *spatialRF* (Benito, 2021). The model was trained using the weighted presence and background records as response variable and the selected environmental variables as model predictors. The model comprised 1000 regression trees, with a minimum node size set to twenty observations. To analyze the model results we first assessed variable permutation importance (Appendix S3). We also assessed partial dependence curves for every predictor and interaction surfaces for the most important pairs of predictors. Finally, we evaluated the predictive performance of the models on independent data via spatial cross-validation on 100 independent spatial folds by computing the median area under the receiver operating characteristics curve (AUC, Fielding and Bell, 1997). Each model was fitted on geographically continuous training folds including 75% of the total training records, and predicted over the remaining data on each iteration.

2.4. Statistical analyses

2.4.1. Polynomial regression

The relationship between habitat suitability and abundance indices was first analyzed using a linear model fitted with a Gaussian distribution and an identity link function. For each abundance index, we investigated the linear relationship between the abundance index and HSI (HSIm), and then we tested the same relationship, adding the HSI quadratic term (HSI2m). For the four abundance indices, we ranked three models (null, linear, and quadratic model) based on Akaike Information Criteria (AIC, Burnham and Anderson, 2002). We selected the best model, i.e. the one with the lower AIC, or the model with fewer parameters if the delta AIC was lower than two between the two models (Arnold, 2010), and checked the residuals of the selected models. All analyses, abundance indices were log-transformed, except for the trend index.

2.4.2. Quantile regression

Statistical distributions of ecological data, such as abundances, often show unequal variation (i.e. more than one slope describing the relationship between a response variable and measured predictor variables). This pattern might be due to complex interactions between factors affecting organisms that cannot all be measured or accounted for in statistical models (Cade and Noon, 2003). The quantile regression method (Koenker and Bassett, 1978) facilitates applying linear regression on a whole data set, taking into account the values above a selected quantile. This method can be seen as an extension of standard linear regression models, as it allows regressing on quantiles rather than on the mean. The ability to study, at any quantile, the linear relationship between two variables provides a complete view of the statistical properties of a sample. Due to expected complex relationship between abundance and HSI (VanDerWal et al., 2009; Jiménez-Valverde et al., 2021), quantile regression may produce better results than the ordinary linear regression approach (Cade and Noon, 2003; Tôrres et al., 2012; Martínez-Gutiérrez et al., 2018).

We used the R package *quantreg* v5.36 (Koenker, 2022) to fit linear quantile regressions between mean abundance and HS and between max abundance and HSIm, to the 50th, 60th, 70th, 80th, 90th, 95th, 97th and 99th percentiles. The R1 measure (weighted sum of absolute residuals) was calculated in each percentile as a local measure of goodness-of-fit (Koenker and Machado, 1999; Acevedo et al., 2017), representing the proportion of variability explained by the predictor variable. All analyses were conducted using R 4.1.2 (R Core Team, 2021).

3. Results

3.1. Habitat Suitability Index

We modelled the habitat suitability of the population of Houbara bustards (HSI) in the fall season in the study area. Eleven non-collinear environmental variables were selected from the set of candidate predictors. The selected predictors were climate variables: temperature seasonality (bio4), precipitation of the warmest quarter (bio18), climate aridity index; the annual range of the Normalized Difference Vegetation Index (NDVI); topographic variables: maximum topographic sun radiation, average topographic sun hours, wetness, position, and diversity; variables representing human presence and impact: human footprint and human accessibility (Appendix S3). According to the permutation importance analysis and the partial dependence curves, aridity, solar radiation, and temperature and precipitation seasonality were the most important predictors, followed by human accessibility and footprint, and the NDVI range. The median of AUC values across the tested spatial folds was 0.924 (median absolute deviation = 0.052), with values ranging from 0.27 to 0.98 over 100 iterations. Over the study area, the mean HSI was 0.78 ± 0.25 (Fig. 1).

3.2. Linear and polynomial regression

We fitted linear and polynomial models for each abundance index (mean, maximum, coefficient of variation and trend), using the HSI as an explaining variable.

For each abundance index, we compared and selected the best model between linear and quadratic models, based on the AIC criterion (Table 1). Linear models were the best models selected for the indices of maximum local abundance and temporal trends. Quadratic models were the best models selected for the indices of mean local abundance and coefficient of variation of local abundance (Table 1).

Results indicated a positive, non-linear effect of the HSI with the local mean abundance over the study period (Table 2, Fig. 2a). The maximum abundance significantly linearly increased with the HSI (Fig. 2b). The relationship between temporal trends of local abundances and HSI was significantly negative (Fig. 2c) but was associated with high dispersion of abundance trends in sites with medium and high HSI. The significant quadratic relationship between the coefficient of variation of local abundances and HSI revealed a non-monotonic variation and the highest variation of abundances for the intermediate HSI (Table 2, Fig. 2d).

3.3. Quantile regression

Quantile regression models showed that the relationship between the HSI and the mean and maximum abundance per pixel was triangular (Fig. 3). Each quantile regression had a significantly positive slope, showing that the upper limit of mean abundance

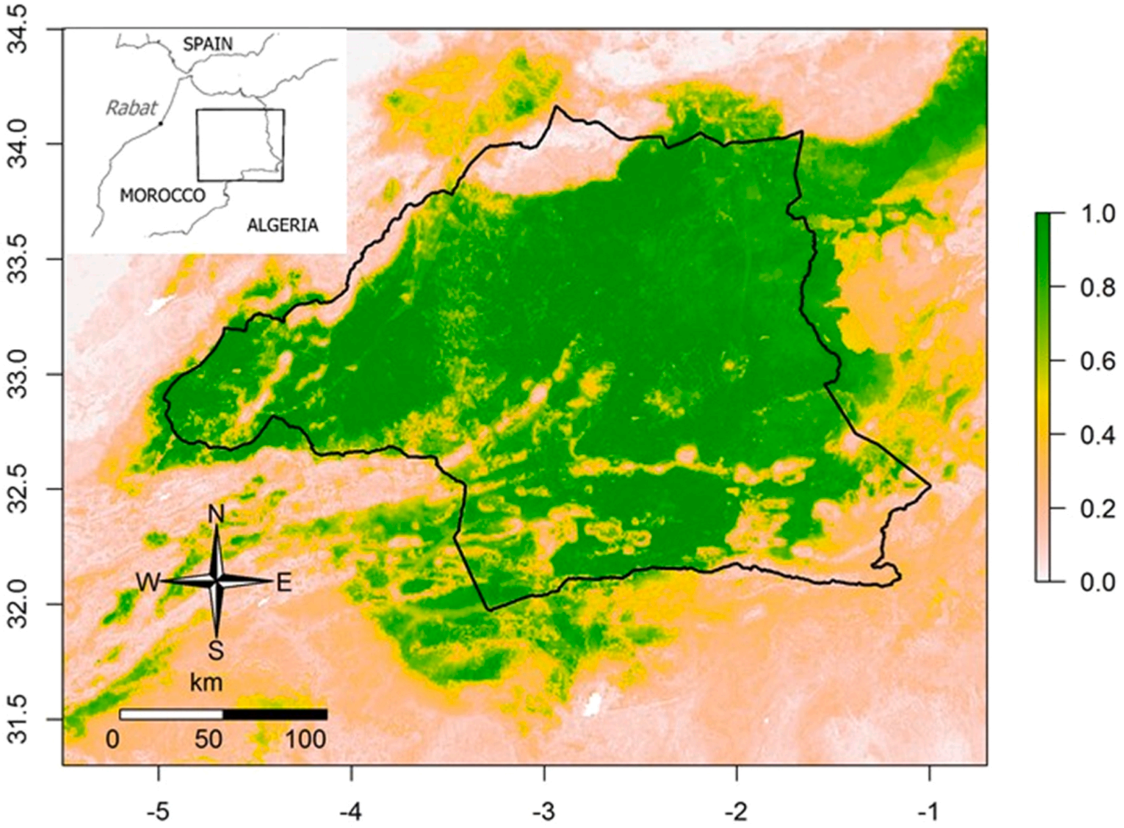

Fig. 1. Map of Habitat Suitability index of the population of the North African Houbara bustard (Chlamydotis undulata undulata) for the fall season in the Eastern study area in Morocco.

Table 1
Comparison by AIC criterion of null, linear and quadratic models tested for relationships between HSI and each abundance index.

	Null model	Linear model	Quadratic model
Mean abundance	2418	2300	**2294**
Max abundance	2686	**2597.2**	2597.4
Coefficient of variation	-1076	-1123	**-1151**
Trend	-1830	**-1871**	-1870

Note: Bold numbers correspond to the selected, most parsimonious models.

Table 2
Summary of significant coefficients and 95% confidence intervals (CIs) of linear and quadratic models for each abundance index. HSI2m represent the quadratic effect of HSIm.

	Linear model	Quadratic model	
	HSIm	**HSIm**	**HSI2m**
Mean abundance	**1.61**	**10.16**	**2.48**
	[1.34, 1.89]	**[8.41, 11.91]**	**[0.73, 4.22]**
Max abundance	**1.65**	**10.38**	1.39
	[1.32, 1.98]	**[8.31, 12.46]**	[− 0.68, 3.47]
Coefficient of variation	**-0.14**	**-0.90**	**-0.69**
	[− 0.18, − 0.10]	**[− 1.15, − 0.66]**	**[− 0.94, − 0.45]**
Trend	**-0.09**	**-0.55**	-0.05
	[− 0.11, − 0.06]	**[− 0.71, − 0.39]**	[− 0.21, 0.11]

Note: Bold numbers indicate significant coefficient (p-value < 0.05).

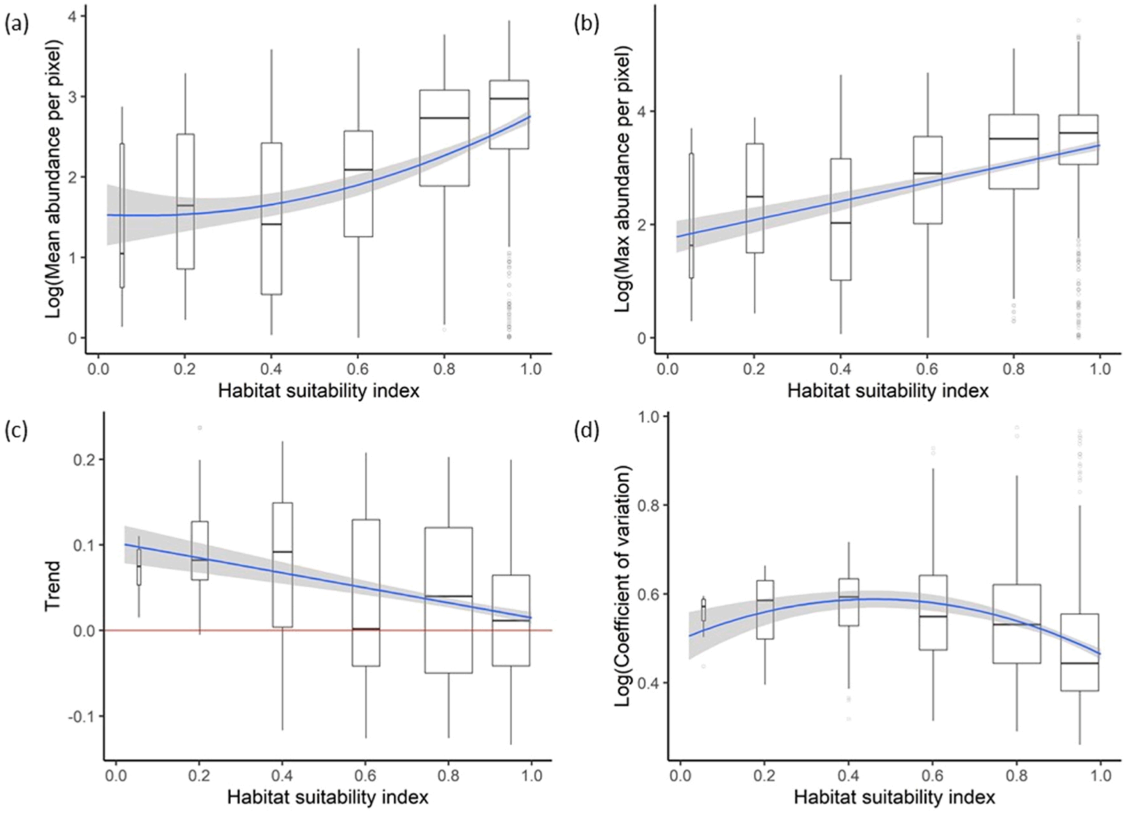

Fig. 2. Relationships between abundance indices (blue lines: predicted model values with CI ± 95% shaded area) and habitat suitability index (HSI), using the best GLM model based on the AIC criterion (linear or polynomial): (a) the mean abundance per pixel (polynomial model) over the study period, (b) the maximum abundance per pixel (linear model) over the study period, (c) the temporal trend of local abundances calculated per pixel (linear model), and (d) the coefficient of temporal variation of abundance associated with each pixel (polynomial model). The boxplots represent the abundance indices distribution for different HSI values summarized in categories.

(Fig. 3a) and maximum abundance (Fig. 3b) increased with increasing HSI. For both abundance indices tested, slopes of quantile regressions were all significantly different from zero and became slightly higher with increasing quantiles, particularly above quantile 0.9 (Appendix S4). In addition, R1 measures (local measure of goodness-of-fit) generally stagnated or decreased with quantiles, but increased for quantiles above 0.9 (Appendix S4). The highest mean and maximum abundance values were observed in pixels associated with the highest HSI values.

4. Discussion

In this study, we examined whether the Habitat Suitability Index (HSI) can predict local abundances in a bird population. In contrast to most previous studies on the demography-HSI relationship, we used average local abundances along with maximum abundances and two indices reflecting their temporal variation over ten consecutive years: the coefficient of variation and the temporal trend of local abundances. Our results indicate a positive association between abundance and HSI. We also found a significant statistical association between habitat suitability and temporal variation in local abundance, suggesting that low and high suitability sites yield lower variation in local abundances than the sites of intermediate quality. However, we found a negative linear relationship between local temporal trend and HSI. Finally, our study indicates the presence of a triangular relationship between HSI and the mean and maximum local abundances. Overall, our results support the hypothesis that HSI obtained from SDMs can reflect the local abundance potentialities of a species and emphasize the importance of investigating this relationship using temporal variation in abundance.

As previously suggested (Muñoz et al., 2015; Jiménez-Valverde et al., 2021), our results indicate that linear regressions tend to mask more complex relationships between abundance and HSI. Studies investigating the linear relationship between local abundance and HSI have reported a generally positive relationship (Tellería et al., 2012; Weber et al., 2017; Lunghi et al., 2018) but not consistently associated with a strong correlation (Bean et al., 2014; Adhikari et al., 2018). In our study, the residuals of the linear models between mean and maximum local abundances with HSI exhibit non-constant variances along the range of predicted values (Appendix S5), thus violating one of the assumptions of linear regressions. The use of alternative methods, such as quantile regression, appeared to be a more appropriate method to analyze this type of triangular relationship (Cade and Noon, 2003; VanDerWal et al., 2009; Acevedo et al., 2017; Jimenez-Valverde et al., 2021). Abundances were consistently low or equal to zero at low quality sites, while they exhibited a wider range of realized abundances at good quality sites.

While a positive relationship exists for both the local mean and maximum abundance vs. HSI relationship, the latter is closer to linearity than the former (Fig. 2). In addition, the predictive power of the linear quantile regression model between mean abundance and HSI decreases with increasing quantiles in contrast to local maximum abundance, which increases at higher quantiles. The predictive power of linear quantile regression seems to be better for quantiles equal to or close to the median (quantile = 0.5) for mean abundance (Appendix S4). As habitat suitability increases, the number of individuals that the site can support becomes larger. Maximum local abundances associated with the most suitable sites were approximately five times higher than at the less suitable sites. The impact of variation in local abundances with habitat suitability is not negligible, especially for a low-density species such as the houbara (0.44 individuals/km^2, Monnier-Corbel et al., 2021), and may have significant effects on population dynamics, through negative density-dependent processes (Monnier-Corbel et al., 2022). Overall, our results are in line with the hypothesis that the upper limit of the triangular relationship indicates the maximum abundance that a population can achieve, and could be interpreted as a surrogate for environmental carrying capacity (VanDerWal et al., 2009; Muñoz et al., 2015; Acevedo et al., 2017).

Our analysis also uncovered a statistical association between habitat suitability and temporal variation in local abundance. In particular, the amount of the inter-annual variation in abundance was substantially reduced in high-quality sites as compared with low-quality sites and sites of intermediate quality (Fig. 2d). Two main types of mechanisms explain the temporal variation in abundance of a population at a point in space: the intrinsic growth of this population and the dispersal of individuals (emigration and immigration). The relative importance of these processes on abundance variation depends on the spatial scale considered and the

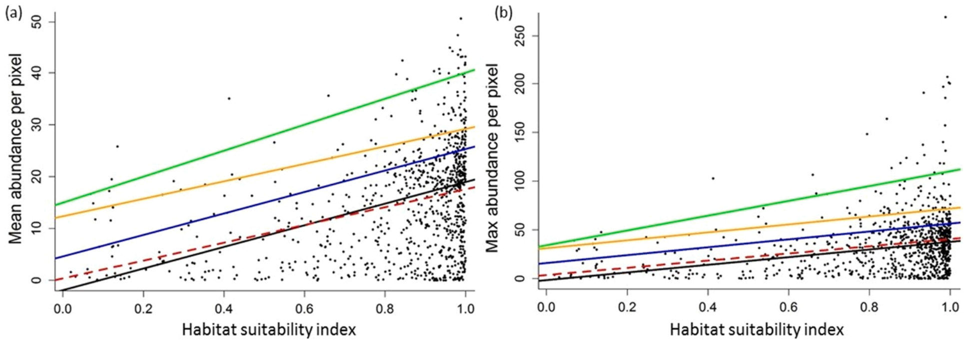

Fig. 3. Relationships between (a) the mean abundance per pixel or (b) the maximum abundance per pixel and the habitat suitability (HS) index, from quantile regression models. The lines represent the linear regression (red dotted line), and different quantiles: the 50th quantile (dark line), the 80th quantile (blue line), the 90th quantile (orange line), the 97th quantile (green line).

species (Brown et al., 1995; Kneitel and Chase, 2004). Habitat selection reflects an individual's preferences, which are shaped by differences in fitness in response to habitat resource heterogeneity (Morris, 1989; Abrams, 2000). Habitat selection is expected to maximize the fitness of individuals in a population and results from demographic processes and individual behavior. Local population density, age, reproductive status, body condition and predation pressure may influence habitat choice and dispersal of individuals from one habitat to another. In high quality sites for houbara, abundances can be maintained to values close to carrying capacity by high attractiveness, positive intrinsic growth rate and density-dependent regulation mechanisms (Monnier-Corbel et al., 2022). For low quality sites that are unattractive and cannot support an increasing population, we also expect to observe low or zero numbers and low temporal variance.

The temporal component of the triangular HSI-abundance relationship was also studied using temporal linear trends of local abundances. As shown in Fig. 2c, the observed local trends are overall positive over the study area, but the slopes also tend to decrease for sites with the highest HSI values, suggesting that some density-dependent regulation may occur at these sites (Monnier-Corbel et al., 2022).

Overall, our results indicate that HSI is related to the temporal variation in abundance in houbara. However, despite the quality of the data set used, our study suffers from methodological limitations. The first limitation is related to our model, the houbara population, and its absence of clear trend at the spatial and temporal scale of the study: from 2011 to 2020 on the Eastern region of Morocco. Over the study period the overall population does not show a clear global trend (positive or negative) at the scale of the study area (Monnier-Corbel et al., 2021). Therefore, using a single relationship was not relevant as the distribution of temporal trend estimates was widely dispersed for medium and higher HSI, showing in those sites, positive and negative trends (Appendix S6). Studying a population with a clear decreasing or increasing trend (see e.g., Acevedo et al., 2017) would have allowed more accurate predictions of the relationship between abundance and HSI. A second limitation is that the trend analysis is based on a meta-analysis (i.e., statistical analysis of statistical objects such as regression slopes), which is intrinsically problematic if the statistical objects analyzed have very different errors. In our particular case, only a very small number of points (34 out of 844) are associated with significant trends. A third limitation of our study, which relates to our general results on the statistical relationship between HSI and abundance, concerns the low variance of HSI over the Eastern study area (see Fig. 1 and discussion in Monnier-Corbel et al., 2022), where habitats are generally highly favorable. Studying an area with more contrasting habitat qualities would have increased the statistical power. Another potential limitation that could have a degree of influence in our results is the use of a single SDM algorithm in our study (Random Forest). Future research could benefit from a better understanding on how various modelling algorithms may yield models showing different relationships with the temporal variation in local abundance.

Finally, in terms of general understanding of the relationship between HSI and demography, the main limitation is the idiosyncratic nature of our study. While the literature indicates contrasting correlations of HSI and mean abundance (Lee-Yaw et al., 2022), our study goes further by looking specifically at variations in abundance. Nevertheless, our results concern a particular, low-density species, which faces specific threats and whose study population is the object of a local restoration program. Because of these particularities, this species benefits from long-term and intensive monitoring providing data sets rarely available to conduct such studies. It is therefore necessary to extend our approach to other systems in order to generalize our findings.

The relationship between habitat suitability provided by SDM and the local abundance of a species has broad implications for conservation actions. The IUCN emphasized the importance of habitat suitability (IUCN/SSC, 2013) as a crucial parameter for translocation success (Wolf et al., 1998). The species-specific habitat suitability can have an essential role in the selection of translocation sites by minimizing translocation risk and ensuring the best possible outcome through the identification of high potential habitats (Osborne and Seddon, 2012). Our study indicates that SDM can predict mean and maximum local species abundances as well as temporally stable sites in terms of abundance variation. Thus, HSI can be interpreted as a proxy of carrying capacity. In addition, HSI can be a tool for optimizing release strategy and improving translocation success by selecting sites with high HSI, associated with high potential abundance and lower temporal variation. Beyond the field of translocation ecology, using SDM to infer possible local abundances may be useful for to make predictions at large spatial scales, without the need to determine abundance at all locations while avoiding the need for costly monitoring protocols.

On a more fundamental level, we suggest that future work on the relationship between HSI and abundance should focus on the more mechanistic aspects of this relationship, including studying the links between site attractiveness, carrying capacity and HSI estimated though various approaches (Zajac et al., 2015; Kaky et al., 2020). On one hand, this involves, for example, understanding the links between HSI and individual behavior such as habitat selection or movement. On the other hand, in some species, carrying capacity can be estimated using proxies such as the number of potential breeding sites in an area, or the amount of resources available in the environment (Goss-Custard et al., 2002; David et al., 2015; Jooste et al., 2013). It would therefore be possible to study the relationship between mechanistic estimators of the carrying capacity of an environment and HSI.

Declaration of Competing Interest

The authors declare that they have no known competing financial interests or personal relationships that could have appeared to influence the work reported in this paper.

Data availability

Data will be made available on request.

Acknowledgements

Funds and samples used in this study were provided by the International Fund for Houbara Conservation (IFHC). We are grateful to His Highness Sheikh Mohamed bin Zayed Al Nahyan, President of the United Arab Emirates and founder of the IFHC, His Highness Sheikh Theyab bin Mohamed Al Nahyan, Chairman of the IFHC, and His Excellency Mohammed Ahmed Al Bowardi, Deputy Chairman, for their support. This study was conducted under the guidance of Reneco International Wildlife Consultants LLC, a consulting company that manages the IFHC's conservation programmes. We thank Dr Frédéric Lacroix, Managing Director of Reneco, as well as Reneco employees who participated in data collection, specifically from the Ecology division Thibault Dieuleveut, Christelle Lucas, Cedric Ferlat, and Eric le Nuz. We thank Stéphane Robin for his advice on our statistical analysis.

Appendix A. Supporting information

Supplementary data associated with this article can be found in the online version at doi:10.1016/j.gecco.2023.e02442.

References

Abrams, P.A., 2000. The evolution of predator-prey interactions: theory and evidence. Annu. Rev. Ecol. Syst. 79–105.

Acevedo, P., Ferreres, J., Escudero, M.A., Jimenez, J., Boadella, M., Marco, J., 2017. Population dynamics affect the capacity of species distribution models to predict species abundance on a local scale. Divers. Distrib. 23 (9), 1008–1017.

Adhikari, D., Mir, A.H., Upadhaya, K., Iralu, V., Roy, D.K., 2018. Abundance and habitat-suitability relationship deteriorate in fragmented forest landscapes: a case of Adinandra griffithii Dyer, a threatened endemic tree from Meghalaya in northeast India. Ecol. Process. 7 (1), 1–9.

Arnold, T.W., 2010. Uninformative parameters and model selection using Akaike's Information Criterion. J. Wildl. Manag. 74 (6), 1175–1178.

Bachman, S.P., Field, R., Reader, T., Raimondo, D., Donaldson, J., Schatz, G.E., Lughadha, E.N., 2019. Progress, challenges and opportunities for Red Listing. Biol. Conserv. 234, 45–55.

Bacon, L. (2017). Etude des paramètres de reproduction et de la dynamique d'une population renforcée d'outardes Houbara nord-africaines (Chlamydotis undulata undulata) au Maroc (Ph.D. thesis). National Museum of Natural History, Paris.

Bacon, L., Hingrat, Y., Jiguet, F., Monnet, A.C., Sarrazin, F., Robert, A., 2017. Habitat suitability and demography, a time-dependent relationship. Ecol. Evol. 7 (7), 2214–2222.

Baer, K.C., Maron, J.L., 2020. Ecological niche models display nonlinear relationships with abundance and demographic performance across the latitudinal distribution of Astragalus utahensis (Fabaceae). Ecol. Evol. 10 (15), 8251–8264.

Bean, W.T., Prugh, L.R., Stafford, R., Butterfield, H.S., Westphal, M., Brashares, J.S., 2014. Species distribution models of an endangered rodent offer conflicting measures of habitat quality at multiple scales. J. Appl. Ecol. 51 (4), 1116–1125.

Benito, B.M., 2021. spatialRF: easy spatial regression with random forest. R. Package Version 1. 1. 0. https://doi.org/10.5281/zenodo.4745208. ⟨https://blasbenito.github.io/spatialRF/⟩.

BirdLife International. (2016). Chlamydotis undulata. The IUCN Red List of Threatened Species 2016: e.T22728245A90341807.

Boyce, M.S., McDonald, L.L., 1999. Relating populations to habitats using resource selection functions. Trends Ecol. Evol. 14 (7), 268–272.

Brown, J.H., 1984. On the relationship between abundance and distribution of species. Am. Nat. 124 (2), 255–279.

Brown, J.H., Mehlman, D.W., Stevens, G.C., 1995. Spatial variation in abundance. Ecology 76, 2028-204.

Buckland, S.T., Elston, D.A., 1993. Empirical models for the spatial distribution of wildlife. J. Appl. Ecol. 478–495.

Burnham, K.P., Anderson, D.R., 2002. A practical information-theoretic approach. Model Sel. Multimodel Inference 2, 70–71.

Cade, B.S., Noon, B.R., 2003. A gentle introduction to quantile regression for ecologists. Front. Ecol. Environ. 1 (8), 412–420.

Cardoso, P., Borges, P.A., Triantis, K.A., Ferrández, M.A., Martín, J.L., 2012. The underrepresentation and misrepresentation of invertebrates in the IUCN Red List. Biol. Conserv. 149 (1), 147–148.

Carnaval, A.C., Moritz, C., 2008. Historical climate modelling predicts patterns of current biodiversity in the Brazilian Atlantic forest. J. Biogeogr. 35 (7), 1187–1201.

Carrascal, L.M., Moreno, Á.C., Delgado, A., Suárez, V., Trujillo, D., 2017. Habitat suitability—density relationship in an endangered woodland species: the case of the Blue Chaffinch (Fringilla polatzeki). PeerJ 5, e3771.

Cowie, R.H., Bouchet, P., Fontaine, B., 2022. The sixth mass extinction: fact, fiction or speculation? Biol. Rev.

David, G.S., Carvalho, E.D.D., Lemos, D., Silveira, A.N., Dall'Aglio-Sobrinho, M., 2015. Ecological carrying capacity for intensive tilapia (Oreochromis niloticus) cage aquaculture in a large hydroelectrical reservoir in Southeastern Brazil. Aquac. Eng. 66, 30–40.

Downs, J.A., Gates, R.J., Murray, A.T., 2008. Estimating carrying capacity for sandhill cranes using habitat suitability and spatial optimization models. Ecol. Model. 214 (2–4), 284–292.

Elith, J., Leathwick, J.R., 2009. Species distribution models: ecological explanation and prediction across space and time. Annu. Rev. Ecol. Evol. Syst. 40, 677–697.

Fielding, A.H., Bell, J.F., 1997. A review of methods for the assessment of prediction errors in conservation presence/absence models. Environ. Conserv. 24 (1), 38–49.

Fox, J., Monette, G., 1992. Generalized collinearity diagnostics. J. Am. Stat. Assoc. 87 (417), 178–183.

Gianpasquale, C., 2017. Landscape structure influencing the spatial distribution of the Short-toed Treecreeper Certhia brachydactyla in a Mediterranean agroecosystem. Avian Biol. Res. 10 (1), 49–57.

Goriup, P.D., 1997. The world status of the houbara bustard Chlamydotis undulata. Bird. Conserv. Int. 7, 373–397.

Goss-Custard, J.D., Stillman, R.A., West, A.D., Caldow, R.W.G., McGrorty, S., 2002. Carrying capacity in overwintering migratory birds. Biol. Conserv. 105 (1), 27–41.

Guyondet, T., 2015. Climate change influences carrying capacity in a coastal embayment dedicated to shellfish aquaculture. Estuaries Coasts 38 (5), 1593–1618.

Hardouin, L.A., Hingrat, Y., Nevoux, M., Lacroix, F., Robert, A., 2015. Survival and movement of translocated houbara bustards in a mixed conservation area. Anim. Conserv. 18 (5), 461–470.

Hingrat, Y., Ysnel, F., Jalme, M.S., Le Cuziat, J., Béranger, P.M., Lacroix, F., 2007. Assessing habitat and resource availability for an endangered desert bird species in eastern Morocco: the Houbara Bustard. Biodivers. Conserv. 16 (3), 597–620.

IUCN/SSC. (2013). Guidelines for reintroductions and other conservation translocations. Version 1.0. Gland, Switzerland. Available from http://www.issg.org/pdf/publications/RSG_ISSG-Reintroduction-Guidelines-2013.pdf.

IUCN/SSC. (2017). Guidelines for Species Conservation Planning. Version 1.0. Gland, Switzerland: IUCN. xiv + 114 pp.

Jiménez-Valverde, A., Aragón, P., Lobo, J.M., 2021. Deconstructing the abundance–suitability relationship in species distribution modelling. Glob. Ecol. Biogeogr. 30 (1), 327–338.

Jooste, E., Hayward, M.W., Pitman, R.T., Swanepoel, L.H., 2013. Effect of prey mass and selection on predator carrying capacity estimates. Eur. J. Wildl. Res. 59 (4), 487–494.

Kaky, E., Nolan, V., Alatawi, A., Gilbert, F., 2020. A comparison between Ensemble and MaxEnt species distribution modelling approaches for conservation: A case study with Egyptian medicinal plants. Ecol. Inform. 60, 101150.

Kearney, M., Porter, W., 2009. Mechanistic niche modelling: combining physiological and spatial data to predict species' ranges. Ecol. Lett. 12 (4), 334–350.

Kneitel, J.M., Chase, J.M., 2004. Trade-offs in community ecology: linking spatial scales and species coexistence. Ecol. Lett. 7 (1), 69–80.

Koenker, R., 2022. quantreg: quantile regression. R. Package Version 5, 88.

Koenker, R., Bassett Jr, G., 1978. Regression quantiles. Econometrica: journal of the Econometric. Economet. J. EconometricSoc. 33–50.

Koenker, R., Machado, J.A., 1999. Goodness of fit and related inference processes for quantile regression. J. Am. Stat. Assoc. 94 (448), 1296–1310.

Lacroix, F., Seabury, J., Al Bowardi, M., Renaud, J., 2003. The Emirates Center for Wildlife Propagation: comprehensive strategy to secure self-sustaining wild populations of Houbara Bustard (Chlamydotis undulata undulata) in Eastern Morocco. Houbara N. 5, 2.

Lee-Yaw, J., McCune, L., J, Pironon, S., Sheth, N., S, 2022. Species distribution models rarely predict the biology of real populations. Ecography 2021 (6), e05877.

Liu, C., Wang, Q., Zhao, W., Liu, H., Tang, X., Zhang, Z., Zhou, J., 2017. Assessing the carrying capacity of Perinereis aibuhitensis in a Chinese estuarine wetland using a GIS-based habitat suitability index model. Aquac. Environ. Interact. 9, 347–360.

Lunghi, E., Manenti, R., Mulargia, M., Veith, M., Corti, C., Ficetola, G.F., 2018. Environmental suitability models predict population density, performance and body condition for microendemic salamanders. Sci. Rep. 8 (1), 1–11.

Martínez-Gutiérrez, P.G., Martínez-Meyer, E., Palomares, F., Fernández, N., 2018. Niche centrality and human influence predict rangewide variation in population abundance of a widespread mammal: the collared peccary (Pecari tajacu). Divers. Distrib. 24 (1), 103–115.

McKeon, G.M., Stone, G.S., Syktus, J.I., Carter, J.O., Flood, N.R., Ahrens, D.G., Day, K.A., 2009. Climate change impacts on northern Australian rangeland livestock carrying capacity: a review of issues. Rangel. J. 31 (1), 1–29.

Miller, D.L., Burt, M.L., Rexstad, E.A., Thomas, L., 2013. Spatial models for distance sampling data: recent developments and future directions. Methods Ecol. Evol. 4 (11), 1001–1010.

Monnet, A.C., Hardouin, L.A., Robert, A., Hingrat, Y., Jiguet, F., 2015. Evidence of a link between demographic rates and species habitat suitability from post release movements in a reinforced bird population. Oikos 124 (8), 1089–1097.

Monnier-Corbel, A., Monnet, A.C., Bacon, L., Benito, B.M., Robert, A., Hingrat, Y., 2022. Density-dependence of reproductive success in a Houbara bustard population. Glob. Ecol. Conserv. 35, e02071.

Monnier-Corbel, A., Monnet, A.C., Hingrat, Y., Robert, A., 2021. Patterns of abundance reveal evidence of translocation and climate effects on Houbara bustard population recovery. Anim. Conserv. 25 (2), 297–310.

Morris, D.W., 1989. Density-dependent habitat selection: testing the theory with fitness data. Evolut. Ecol. 3 (1), 80–94.

Muñoz, A.R., Jiménez-Valverde, A., Márquez, A.L., Moleón, M., Real, R., 2015. Environmental favourability as a cost-efficient tool to estimate carrying capacity. Divers. Distrib. 21 (12), 1388–1400.

O'brien, R.M., 2007. A caution regarding rules of thumb for variance inflation factors. Qual. Quant. 41 (5), 673–690.

Osborne, P.E., Seddon, P.J., 2012. Selecting suitable habitats for reintroductions: variation, change and the role of species distribution modelling. Reintroduction Biol.: Integr. Sci. Manag. 1, 73–104.

R Core Team, 2021. R: A language and environment for statistical computing. R Foundation for Statistical Computing, Vienna, Austria. URL. https://www.R-project.org/.

Ready, J., Kaschner, K., South, A.B., Eastwood, P.D., Rees, T., Rius, J., Froese, R., 2010. Predicting the distributions of marine organisms at the global scale. Ecol. Model. 221 (3), 467–478.

Régnier, C., Achaz, G., Lambert, A., Cowie, R.H., Bouchet, P., and Fontaine, B. (2015). Mass extinction in poorly known taxa. Proceedings of the National Academy of Sciences, 112(25), 7761–7766.

Regos, A., Tapia, L., Gil-Carrera, A., Domínguez, J., 2021. Caution is needed when using niche models to infer changes in species abundance: the case of two sympatric raptor populations. Animals 11 (7), 2020.

Svenning, J.C., Fløjgaard, C., Marske, K.A., Nógues-Bravo, D., Normand, S., 2011. Applications of species distribution modeling to paleobiology. Quat. Sci. Rev. 30 (21–22), 2930–2947.

Tellería, J.L., Santos, T., Refoyo, P., Muñoz, J., 2012. Use of ring recoveries to predict habitat suitability in small passerines. Divers. Distrib. 18 (11), 1130–1138.

Thuiller, W., Münkemüller, T., Schiffers, K.H., Georges, D., Dullinger, S., Eckhart, V.M., Schurr, F.M., 2014. Does probability of occurrence relate to population dynamics? Ecography 37 (12), 1155–1166.

Tôrres, N.M., De Marco, P., Santos, T., Silveira, L., de Almeida Jácomo, A.T., Diniz-Filho, J.A., 2012. Can species distribution modelling provide estimates of population densities? A case study with jaguars in the Neotropics. Divers. Distrib. 18 (6), 615–627.

Van Couwenberghe, R., Collet, C., Pierrat, J.C., Verheyen, K., Gégout, J.C., 2013. Can species distribution models be used to describe plant abundance patterns? Ecography 36 (6), 665–674.

VanDerWal, J., Shoo, L.P., Graham, C., Williams, S.E., 2009. Selecting pseudo-absence data for presence-only distribution modeling: how far should you stray from what you know? Ecol. Model. 220 (4), 589–594.

Verhulst, P.F., 1838. Notice sur la loi que la population suit dans son accroissement. Corresp. Math. Phys. 10, 113–126.

Weber, M.M., Stevens, R.D., Diniz-Filho, J.A.F., Grelle, C.E.V., 2017. Is there a correlation between abundance and environmental suitability derived from ecological niche modelling? A meta-analysis. Ecography 40 (7), 817–828.

Wolf, C.M., Garland Jr, T., Griffith, B., 1998. Predictors of avian and mammalian translocation success: reanalysis with phylogenetically independent contrasts. Biol. Conserv. 86 (2), 243–255.

Wright, M.N., Ziegler, A., 2015. Ranger: a fast implementation of random forests for high dimensional data in C++ and R. arXiv Prepr. arXiv 1508, 04409.

Zajac, Z., Stith, B., Bowling, A.C., Langtimm, C.A., Swain, E.D., 2015. Evaluation of habitat suitability index models by global sensitivity and uncertainty analyses: a case study for submerged aquatic vegetation. Ecol. Evol. 5 (13), 2503–2517.